



Synthesis, crystal structures and magnetic properties of nitronyl nitroxide radical-coordinated copper(II) complexes

Yan-Li Gao¹ · Katsuya Inoue^{2,3}

Received: 8 October 2019 / Accepted: 23 November 2019
© Springer Nature Switzerland AG 2019

Abstract

The coordination compound constructed for nitronyl nitroxide radical NIT-Ph-4-Br and $\text{Cu}^{\text{II}}(\text{hfac})_2(\text{H}_2\text{O})_2$ building blocks (NIT-Ph-4-Br = 2-(4-bromo-phenyl)-4,4,5,5-tetramethylimidazoline-1-oxyl-3-oxide, hfac = hexafluoroacetylacetonato) was successfully synthesized. The single-crystal X-ray diffraction analyses indicated that the complexes $\{(\text{NIT-Ph-4-Br})_2[\text{Cu}(\text{hfac})_2]_3\}$ have centrosymmetric five-spin structures consisting of three $\text{Cu}(\text{II})$ ions bridged by two nitroxide ligands and that they consist of two types of copper atoms, one with a heavily Jahn–Teller distorted (4 + 2) octahedral coordination (Cu^{Oct}) and hfac in *trans*-positions and the other with square pyramidal five-coordinated (Cu^{PyT}) with three hfac oxygen atoms and N–O oxygen atom at the base and the one hfac oxygen atom at the apex. Different geometries of the copper ions are quite important for magnetochemistry. The magnetic susceptibility study of the coordination compound shows strong antiferromagnetic interactions between the metal center and the organic radical.

Introduction

In the past two decades, molecular magnetic materials have attracted scientists' attention due to their potential applications in high-density magnetic memories, quantum computing devices and molecular spintronics [1–6]. Among the variety of molecular magnetic materials with different structures and dimensionalities, the strategy of metal–radical, which is formed by matching paramagnetic organic molecules and transition metal complexes, is still the key way to synthesize and design magnets. Up to now, a variety of organic paramagnetic molecules such as aminoxyl, verdazyl, thiazyl, triazinyl, nindigo, semiquinone and nitroxide radicals have been widely studied in the field of molecular

magnetism [7–15]. Among them, because of their relatively stable and easy-to-obtain derivatives with substituents containing donor atoms, the nitronyl nitroxide (2-(R)-4,4,5,5-tetramethyl-4,5-dihydro-1H-imidazol-1-oxy-3-oxide, NITR) radicals have received more attention of researchers [16–22]. Besides, nitronyl nitroxide family of radicals can act as bidentate ligands with identical N–O coordination groups. Compared with regular diamagnetic ligands, the N–O groups of this kind of radical have weak basicity, so strong acidic partners were needed for ligation to the radical. Thus, it is necessary to utilize the strong electron-withdrawing coligands such as hexafluoroacetylacetonate (hfac) and trifluoroacetylacetonate (tfac) in the metal to improve the weak coordination ability. However, the steric demand of hfac or tfac ancillary ligand can restrict the dimensionality of the resulting metal–radical complex.

Furthermore, copper(II)–nitronyl nitroxide coordination complexes are the best documented and characterized on the basis of their coordination geometry toward development of magnetic materials [23, 24]. The copper(II) ion has a well-defined magnetic orbital of $3d_{x-y}^{22}$; in parallel, the N–O group has an unpaired electron in the molecular π^* orbital. The magnetic coupling parameter J is typically determined as a singlet–triplet energy gap of $2J$ at a $>\text{NO-Cu}$ unit. Generally, an equatorial coordination results in a strong antiferromagnetic metal–radical exchange coupling ($J < 0$), while an

✉ Yan-Li Gao
gaoyanli8503@126.com

✉ Katsuya Inoue
kxi@hiroshima-u.ac.jp

¹ School of Chemistry and Chemical Engineering, Yulin University, Yulin 719000, China

² Department of Chemistry, Hiroshima University, 1-3-1, Kagamiyama, Higashi-Hiroshima, Hiroshima 739-8526, Japan

³ Center for Chiral Science, Hiroshima University, 1-3-1, Kagamiyama, Higashi-Hiroshima, Hiroshima 739-8526, Japan

axial bonding results in a moderate ferromagnetic coupling ($J > 0$) [25–36].

Inspired by these ideas, we synthesized the nitronyl nitroxide ligands (Scheme 1) which can provide an efficient way for magnetic spin exchange, following a detailed study of the structures and magnetism of the metal–radical compounds. In this contribution, we report the crystal structures and magnetic properties of $\{(\text{NIT-Ph-4-Br})_2[\text{Cu}(\text{hfac})_2]_3\}$ obtained from the nitronyl nitroxide radicals and $\text{Cu}^{\text{II}}(\text{hfac})_2$ building blocks.

Experimental

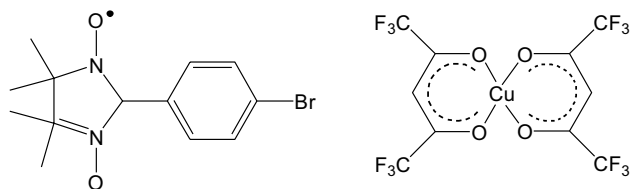
Materials and methods

All reagents were obtained from commercial sources and used without further purification.

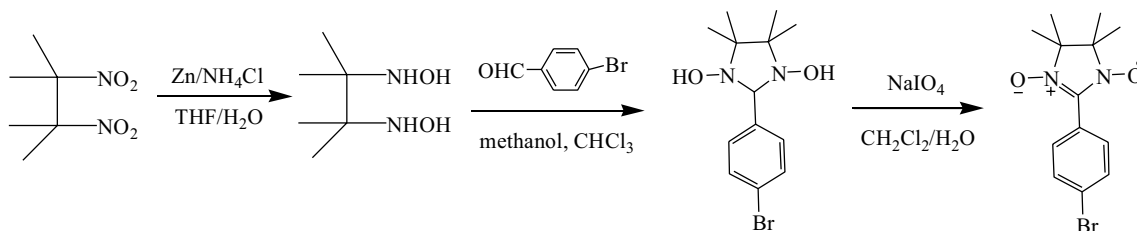
2-(4-Bromo-phenyl)-4,4,5,5-tetramethylimidazoline-1-oxyl-3-oxide radical (NIT-Ph-4-Br) was prepared as reported previously with only minor modifications (Scheme 2) [37, 38].

Preparation of $\text{Cu}(\text{hfac})_2 \cdot 2\text{H}_2\text{O}$

Hfac (1 g, 7.1 mmol) was added to a suspension of $\text{Cu}(\text{CH}_3\text{COO})_2 \cdot \text{H}_2\text{O}$ (0.71 g, 3.55 mmol) in H_2O (17 mL) at room temperature, and then, NaHCO_3 (0.071 g, 0.8 mmol) was added under stirring. After 10 min, a light blue precipitate was obtained and washed three times with *n*-hexane. Then, the light blue solid was dried at 50 °C for three days, and $\text{Cu}(\text{hfac})_2 \cdot 2\text{H}_2\text{O}$ (0.74 g) was obtained. FTIR (KBr, cm^{-1}): 3399(s), 1644(s), 1561(s), 1497(s), 1210(s), 1151(s), 800(s), 766(w), 743(w), 668(s), 590(s).



Scheme 1 Organic radicals NIT-Ph-4-Br and inorganic complexes: $\text{Cu}^{\text{II}}(\text{hfac})_2$



Scheme 2 Synthesis pathway of NIT-Ph-4-Br radical

cm^{-1}): 3399(s), 1644(s), 1561(s), 1497(s), 1210(s), 1151(s), 800(s), 766(w), 743(w), 668(s), 590(s).

Preparation of $\{[(\text{NIT-Ph-4-Br})_2[\text{Cu}(\text{hfac})_2]_3\}$

$\text{Cu}^{\text{II}}(\text{hfac})_2 \cdot (\text{H}_2\text{O})_2$ (1 mmol, 51.5 mg) was dissolved in 10 mL of hot *n*-heptane, and then, the solution was cooled to about 50 °C. NIT-Ph-4-Br (0.05 mmol, 15 mg), dissolved in 2 mL of CHCl_3 , was added to it with constant stirring. The mixed solution was stirred for ca. 3 min and then cooled to room temperature. The filtrate was kept under N_2 stream at room temperature until solid appeared. A few drops of CHCl_3 were added until the solid disappears, and then, the flask was sealed and placed in the refrigerator. After 2–3 days, block-shaped dark blue crystals were obtained, yield 81%. Chemical analyses for $\text{C}_{56}\text{H}_{38}\text{Br}_2\text{Cu}_3\text{N}_4\text{O}_{16}$ are: calculated (%) C: 32.67, H: 1.85, N: 2.72. Found (%): C: 32.84, H: 1.69, N: 2.57. FTIR (KBr, cm^{-1}): 1658(s), 1559(w), 1534(s), 1479(s), 1356(w), 1221(s), 1145(s), 1084(s), 862(s), 798(w), 663(s), 614(s).

General characterizations

Infrared spectra were recorded on a JASCO FT/IR-660 Plus spectrometer by transmission through KBr pellets in the range 400–4000 cm^{-1} . Elemental analyses for C, H, and N were carried out using a PerkinElmer series II CHNS/O Analyzer 2400. The magnetization measurements on the crystalline solids were taken using Quantum Design MPMS-5S and MPMS-2 SQUID magnetometers. The magnetic field was varied from – 50 to 50 kOe and the temperature from 2 to 300 K. The data were corrected for the sample diamagnetism using Pascal's constants [39, 40].

Single-Crystal X-ray diffraction studies

Their X-ray diffraction intensities were collected for the selected single crystals individually mounted on glass fibers at different temperature using a Bruker diffractometer SMART APEX II with a CCD and D8-QUEST with a CMOS area detector. Both employed graphite-monochromated Mo $\text{K}\alpha$ ($\lambda = 0.71073$ Å) radiation. Data reduction

was made using SAINT, and intensities were corrected for absorption by SADABS [41, 42]. The structures were solved by direct methods and refined by full-matrix least squares against F^2 using ShelXL [43]. A part of the hydrogen atoms were located in the difference Fourier maps, and those not found were added at theoretical positions using the riding model. The details can be obtained from the cif files deposited at the Cambridge Crystallographic Data Centre. The crystals and refinements data are summarized in Table 1.

Results and discussion

Crystal structure of complex $\{(\text{NIT-Ph-4-Br})_2[\text{Cu}(\text{hfac})_2]_3\}$

The molecular structures $\{(\text{NIT-Ph-4-Br})_2[\text{Cu}(\text{hfac})_2]_3\}$ were successfully determined by means of X-ray crystallographic analysis at different temperatures. (Table 1 shows selected crystallographic data.) $\{(\text{NIT-Ph-4-Br})_2[\text{Cu}(\text{hfac})_2]_3\}$ crystallizes in the triclinic space group $P-1$ with $Z=1$. The molecular structure is shown in Fig. 1, and it forms a centrosymmetric dimer (Fig. 1b).

Table 1 Crystallographic data and refinement parameters for complexes at 173 K and 90 K

	173(2) K	90(2) K
Formula	$\text{C}_{56}\text{H}_{38}\text{Br}_2\text{Cu}_3\text{F}_{36}\text{N}_4\text{O}_{16}$	$\text{C}_{56}\text{H}_{38}\text{Br}_2\text{Cu}_3\text{F}_{36}\text{N}_4\text{O}_{16}$
fw	2057.35	2057.35
Cryst syst	Triclinic	Triclinic
Space group	$P-1$	$P-1$
a (Å)	11.7115(6)	11.6325(6)
b (Å)	12.5627(6)	12.5658(6)
c (Å)	13.0878(6)	12.9706(6)
α (°)	75.3240(10)	75.2860(10)
β (°)	81.6560(10)	82.2800(10)
γ (°)	89.501(2)	89.2400(10)
V (Å ³)	1842.25(15)	1816.71(15)
D_c (g cm ⁻³)	1.854	1.880
Z	1	1
Refls. total	58,631	47,815
Unique	9179	9039
Param.	641	616
R_{int}	0.0225	0.0216
R_1/wR_2 [$I > 2\sigma(I)$]	0.0302	0.0267
	0.0779	0.0685
R_1/wR_2 (all data)	0.0347	0.0289
	0.0816	0.0699
GoF	1.031	1.033
Completeness	0.995	0.998
Theta (°)	28.35	28.31

As shown in Fig. 1a, the asymmetric unit of complex $\{(\text{NIT-Ph-4-Br})_2[\text{Cu}(\text{hfac})_2]_3\}$ consists of two types of copper atoms, one with a heavily Jahn–Teller distorted (4 + 2) octahedral coordination (Cu^{OCT}) and hfac in *trans*-positions which are occupied by four oxygen atoms (O7, O8) from two hfac units, two oxygen atoms (O1) from two nitroxide ligands, and the other with nearly square pyramidal five-coordinated (Cu^{PYR}) with three hfac oxygen atoms (O3, O5, O6) and the N–O (O2) at the base and one hfac oxygen atom (O4) at the apex. The asymmetric unit of $\{(\text{NIT-Ph-4-Br})_2[\text{Cu}(\text{hfac})_2]_3\}$ consists of one radical, half a Cu^{OCT} (Cu1) and one Cu^{PYR} (Cu2). The whole molecule has five localized $S = 1/2$ spins, which form a zigzag linear spin system along the copper–radical–copper–radical–copper array. The molecular structure consists of alternating metal–radical units. The radical plays a key role in establishing this zero-dimensional structure, acting as a bidentate ligand to connect the metal centers. In addition, there are two slightly longer intermolecular interactions $\text{N2} \cdots \text{O2} \cdots \text{O2} \cdots \text{N2} = 3.540(1)$ Å and $\text{Br1} \cdots \text{Br1} = 3.333(1)$ Å, which bridge the molecule into a layer structure as shown in Fig. 2.

Selected bond lengths and angles are listed in Table 2. For the six-coordinated octahedral copper(II) ions, the apical $\text{Cu1} \cdots \text{O1}$ bond lengths are 2.572(1) Å, while the equatorial $\text{Cu} \cdots \text{O}$ bonds are much shorter than the apical bonds (the $\text{Cu1} \cdots \text{O}$ distances are ~ 1.92 Å), as shown in Figure 3a. Furthermore, the $\text{Cu1} \cdots \text{O1}$ distance was longer compared with typical copper(II)–radical bond lengths (> 2.3 Å) [44–47]. For the square pyramidal five-coordinated copper(II) ions, the apical $\text{Cu2} \cdots \text{O4}$ bond lengths are 2.202(1) Å, while the equatorial $\text{Cu2} \cdots \text{O}$ bond distances range from 1.923 to 1.961 Å, as shown in Figure 3b. Furthermore, $\text{Cu2} \cdots \text{O2}$ bond distance is 1.951(1) Å, which is a typical length for a copper(II)–nitroxide equatorial coordinate bond (1.93–2.03 Å) [46–49]. The bond distances of uncoordinated N–O (1.266(2) Å) are shorter than those of the coordinated ones (1.306(2) Å). In addition, the angles of $\text{N1} \cdots \text{O1} \cdots \text{Cu1}$ and $\text{N2} \cdots \text{O2} \cdots \text{Cu2}$ are 161.56(1)° and 118.14(9)°, respectively. The $\text{O1} \cdots \text{N1} \cdots \text{C3} \cdots \text{N2} \cdots \text{O2}$ is almost planar. The dihedral angle between nitronyl nitroxide and the benzene ring is 38.7°. The molecular arrangement of complex $\{(\text{NIT-Ph-4-Br})_2[\text{Cu}(\text{hfac})_2]_3\}$ is shown in Fig. 2, the nearest intramolecular metal–metal contacts give a $\text{Cu} \cdots \text{Cu}$ distance of 7.759(1) Å, while the intermolecular $\text{Cu} \cdots \text{Cu}$ distance is 6.658(1) Å. The distance of the two corresponding radicals from adjacent molecules is 3.54 Å. No meaningful interdimer interaction, such as a π – π stacking or an interaction through counteranion, was observed in the crystal structures. Thus, the interdimer magnetic interaction is negligible for magnetic analysis.

Fig. 1 Molecular structure of **a** asymmetric unit and **b** trinuclear unit of $\{(NIT-Ph-4-Br)_2[Cu(hfac)_2]_3\}$ with ellipsoids at 50% probability level. Fluorine and hydrogen atoms are omitted for clarity

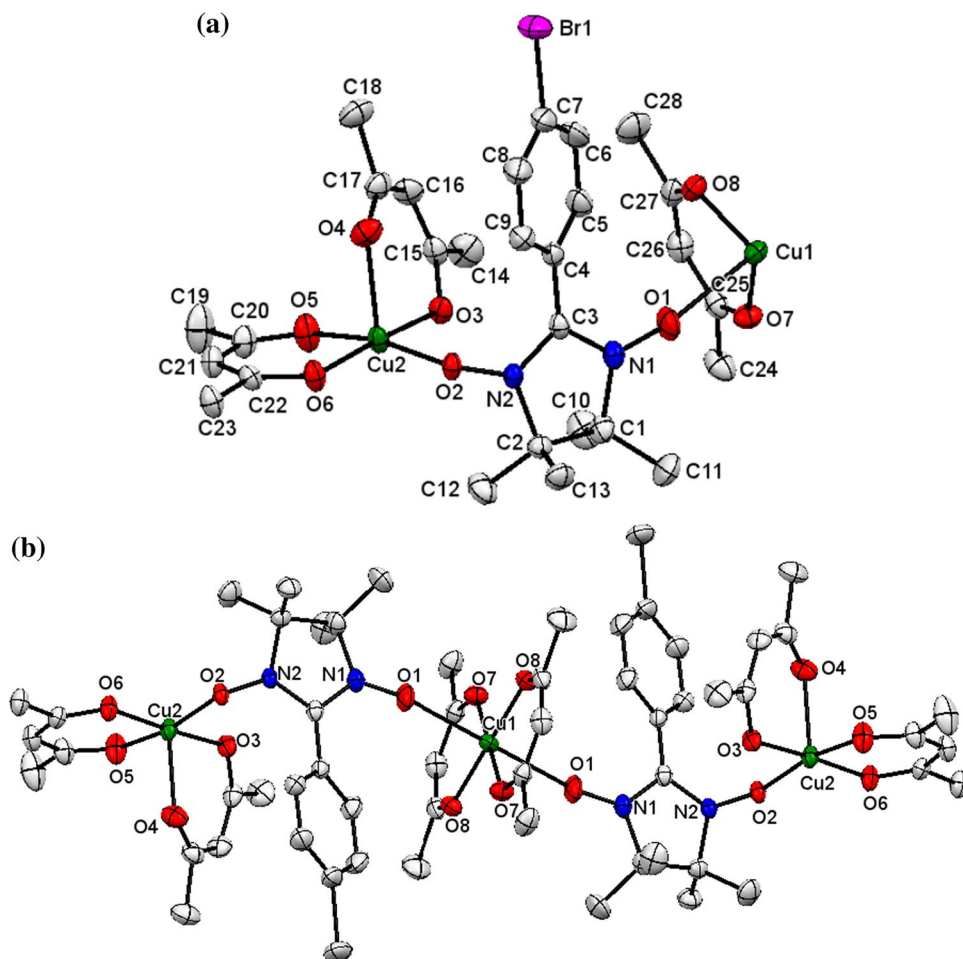


Fig. 2 Crystal packing of complex $\{(NIT-Ph-4-Br)_2[Cu(hfac)_2]_3\}$ showing the O...O (blue) and Br...Br (black) interchain short contacts. Fluorine and hydrogen atoms are omitted for clarity

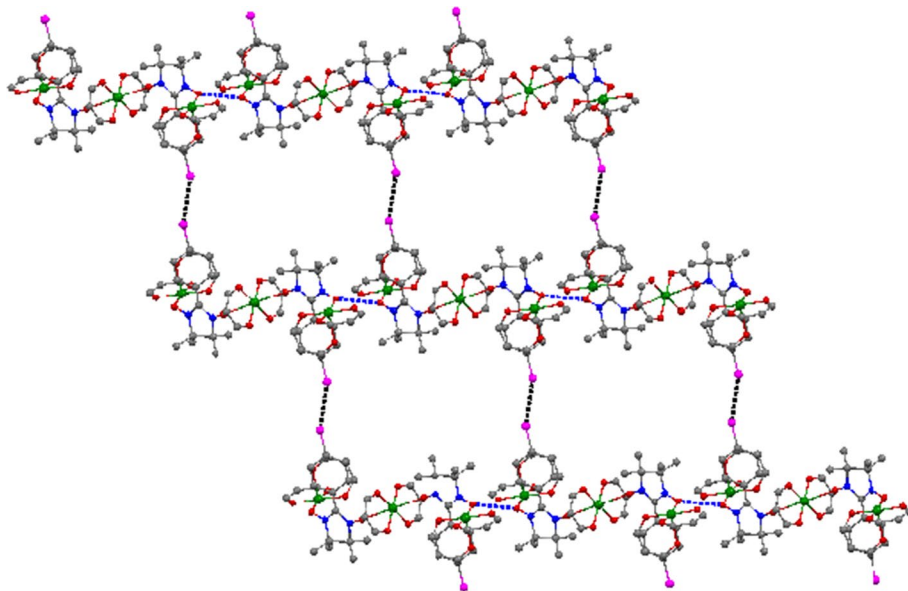
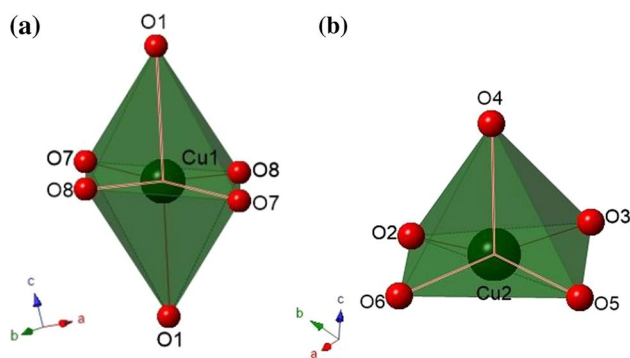


Table 2 Selected bond lengths [Å] and angles [°] for {(NIT-Ph-4-Br)₂[Cu(hfac)₂]₃} at 173 K

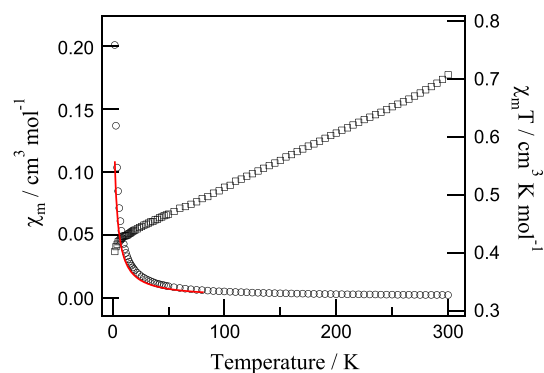
Bond lengths [Å]	
N1–O1 1.266(2)	Cu2–O5 1.961(1)
N2–O2 1.306(2)	Cu2–O6 1.923(1)
Cu1–O1 2.572(1)	Cu2–O7 1.926(1)
Cu2–O2 1.951(1)	Cu2–O8 1.916(1)
Cu2–O3 1.936(2)	Cu2–O6 1.923(1)
Cu2–O4 2.202(1)	C7–Br1 1.930(3)
Angles [°]	
N1 O1 Cu1 161.56(1)	O1–Cu1–O7 89.39(1)
N2 O2 Cu2 118.14(9)	O1–Cu1–O8 99.27(1)
O2 Cu2 O5 167.36(6)	O1 N1 C3 125.49(15)
O2 Cu2 O4 98.25(5)	O1 N1 C1 121.73(14)
O3 Cu2 O2 93.28(5)	O2 N2 C2 120.98(12)
O3 Cu2 O5 85.62(5)	O2 N2 C3 125.39(13)
O3 Cu2 O4 89.67(5)	N2 C3 N1 107.90(14)
O6 Cu2 O2 87.61(5)	C22 O6 Cu2 123.89(10)
O6 Cu2 O3 175.41(5)	C27 O8 Cu1 124.57(11)
O6 Cu2 O5 92.53(5)	C25 O7 Cu1 124.50(11)
O6 Cu2 O4 94.67(5)	C20 O5 Cu2 124.33(11)
O5 Cu2 O4 94.33(6)	C17 O4 Cu2 118.79(12)
O8 Cu1 O7 92.87(5)	C15 O3 Cu2 121.40(11)
O2 N2 C3 125.39(13)	C13–O4–Cu1 124.1(2)
O5 Cu2 O4 94.33(6)	C16–O5–Cu1 123.47(19)
O8 Cu1 O7 92.87(5)	C18–O6–Cu1 124.7(2)
C15 O3 Cu2 121.40(11)	

**Fig. 3** Octahedral structure of Cu1 (a) and square pyramidal structure of Cu2 (b)

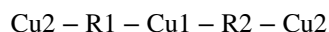
Magnetic Properties

The temperature-dependent magnetic susceptibilities of {(NIT-Ph-4-Br)₂[Cu(hfac)₂]₃} were measured in the temperature range 2–300 K in an external magnetic field of 10 kOe, and the data were corrected for the diamagnetism of the components.

Magnetic data for {(NIT-Ph-4-Br)₂[Cu(hfac)₂]₃} are shown in Fig. 4 as χ_m versus T and $\chi_m T$ versus T . For the

**Fig. 4** Temperature dependence of χ_m (circular) and $\chi_m T$ (square) for complex {(NIT-Ph-4-Br)₂[Cu(hfac)₂]₃}

value of $\chi_m T$ (square), at room temperature the value is 0.71 cm³ K mol⁻¹, which is obviously lower than the theoretical value (1.875 cm³ K mol⁻¹) for an uncoupled system of three copper(II) ($S = 1/2$, $\chi_m T = 0.375$ cm³ K mol⁻¹) plus two radicals ($S = 1/2$, $\chi_m T = 0.375$ cm³ K mol⁻¹), assuming $g = 2$, indicating the existence of strong antiferromagnetic interactions within the compound [48, 49]. With reduction in temperature, $\chi_m T$ sharply decreases to reach a value of 0.40 cm³ K mol⁻¹, which is close to a spin value for $S = 1/2$ with $g = 2$. The effective expression for calculating the susceptibility of the five-spin system has not been found [50, 51]. And, based on the crystal data and the comparison with magnetic properties of other well-understood copper–radical complexes [50–55], the $\chi_m T - T$ curves for this complex can be rationalized qualitatively in term of an approximate model shown as follows:



In this model, we presume that the interactions between Cu1 and R1 and Cu1 and R2 are very small in this complex, while the interactions of Cu2–R1 and Cu2–R2 are strongly antiferromagnetic, because it has been found that two spins will have different coupling phenomena in the coordination environment of copper(II): When the N–O occupies an equatorial position, the spins are strongly coupled in an antiferromagnetic way with $J > 500$ cm⁻¹ ($\hat{H} = J\hat{S}_i\hat{S}_j$) [49, 53]; when the nitroxide occupies an axial position, a weak coupling is found [49]. Therefore, the monotonous decrease in $\chi_m T$ with the decrease in temperature should be ascribed to the very strong antiferromagnetic interaction between the Cu2–R1 and the Cu2–R2. The minimum of $\chi_m T$ of 0.40 cm³ K mol⁻¹ at 2.0 K is close to an uncoupled Cu(II) ion ($S = 1/2$, 0.375 cm³ K mol⁻¹), which may be due to the very strong antiferromagnetic interactions between Cu2 and radicals, which leads to complete spin cancellation. It can also be proved by fitting the susceptibilities (circular) by the Curie–Weiss law (red curve). In the Curie–Weiss fit

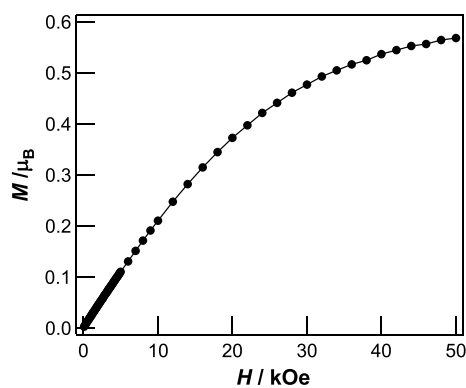


Fig. 5 Isothermal magnetization at 2 K of $\{(\text{NIT-Ph-4-Br})_2[\text{Cu}(\text{hfac})_2]_3\}$

we obtain $C = 0.516 \text{ cm}^3 \text{ K mol}^{-1}$, corresponding to a spin $S = 1/2$ with $g = 2.34$, proving the very strong antiferromagnetic interactions in the systems as expected, which is similar to those of other reported complexes [49–51].

The magnetization versus field curve obtained at 2 K is depicted in Fig. 5. At a magnetic field of 50 kOe, the magnetization reaches a maximum of $0.56 \text{ N}\mu_{\text{B}}$, which is overall smaller than the expected value.

Conclusion

The centrosymmetric complex $\{(\text{NIT-Ph-4-Br})_2[\text{Cu}(\text{hfac})_2]_3\}$ based on copper(II) and nitronyl nitroxide radicals was successfully prepared. The single-crystal structures show that two radicals are bridges linking three Cu(II) ions to form five-spin systems. The magnetic measurements indicate that the complex exhibited antiferromagnetic interactions between Cu(II) ions and radicals. Their magneto-structural correlations were explained based on the crystal structures.

Supplementary data

CCDC contains the supplementary crystallographic data for this paper (1959819 for 90 K and 1959820 for 173 K). The data can be obtained free of charge from The Cambridge Crystallographic Data Centre via www.ccdc.cam.ac.uk/structures.

Acknowledgment This work was supported by (a) a Grant-in-Aid for Scientific Research (S) (No. 25220803) “Toward a New Class Magnetism by Chemically-controlled Chirality,” (b) a National Nature Science Foundation of China (No. 51762042), (c) Shaanxi Provincial Science and Technology Department Innovative Talent Promotion Plan Project of China (No. 2018KJXX-078) and (d) Doctoral Scientific Research Foundation of Yulin university (18GK24).

References

- Itoh K, Kinoshita M (eds) (2000) Molecular magnetism, new magnetic materials. Gordon Breach-Kodansha, Tokyo
- Blundell SJ, Pratt FL (2004) *J Phys: Condens Matter* 16:R771–R828
- Gatteschi D, Sessoli R, Villain J (2006) Molecular nanomagnets. Oxford University Press, Oxford
- Sorace L, Benelli C, Gatteschi D (2011) *Chem Soc Rev* 40:3092–3104
- Gutlich P, Garcia Y, Goodwin HA (2000) *Chem Soc Rev* 29:419–427
- Kurmoo M (2009) *Chem Soc Rev* 38:1353–1379
- Demir S, Jeon IR, Long JR, Harris TD (2015) *Coord Chem Rev* 149:289–290
- Ratera JV (2012) *Chem Soc Rev* 41:303–349
- Brook DJR (2015) *Comments Inorg Chem* 35:1–17
- Preuss KE (2015) *Coord Chem Rev* 49:289–290
- Morgan IS, Mansikkamäki A, Zissimou GA, Koutentis PA, Rouzières M, Clérac R, Tuononen HM (2015) *Chem Eur J* 21:15843–15851
- Morgan IS, Peuronen A, Hänninen MM, Reed RW, Clérac R, Tuononen HM (2014) *Inorg Chem* 53:33–35
- Fortier S, Le Roy JJ, Chen CH, Vieru V, Murugesu M, Chibotaru LF, Mindiola DJ, Caulton KG (2013) *J Am Chem Soc* 135:14670–14678
- Miller JS (2011) *Chem Soc Rev* 40:3266–3296
- Shultz DA, Miller JS, Drillon M (eds) (2002) Magnetism: molecules to materials II: molecule-based materials. Wiley-VCH, Weinheim, pp 281–304
- Witt A, Heinemann FW, Khusniyarov MM (2015) *Chem Sci* 6:4599–4609
- Ocharenko V (2010) Stable radicals. Wiley, ch. 13
- Miller JS, Drillon M (2003) Magnetism: Molecules to Materials II: Molecule-Based Materials, Wiley-VCH Verlag GmbH & Co, ch. 1
- Mckinnon SDJ, Patrick BO, Lever ABP, Hicks RG (2013) *Inorg Chem* 52:8053–8066
- Wu J, MacDonald DJ, Clérac R, Jeon IR, Jennings M, Lough AJ, Britten J, Robertson C, Dube PA, Preuss KE (2012) *Inorg Chem* 51:3827–3839
- Kaszub W, Marino A, Lorenc M, Collet E, Bagryanskaya EG, Tretyakov EV, Ovcharenko VI, Fedin MV (2014) *Angew Chem Int Ed* 53:10636–10640
- Wang J, Li JN, Zhang SL, Zhao XH, Shao D, Wang XY (2016) *Chem Commun* 52:5033–5036
- Caneschi A, Gatteschi D, Sessoli R, Rey P (1989) *Acc Chem Res* 22:392–398
- Caneschi A, Gatteschi D, Rey P (1991) *Prog Inorg Chem* 39:331–334
- Dickman MH, Doedens RJ (1981) *Inorg Chem* 20:2677–2681
- Porter LC, Ickmann MH, Doedens RJ (1983) *Inorg Chem* 22:1962–1964
- Porter LC, Doedens RJ (1985) *Inorg Chem* 24:1006–1010
- Lim YY, Drago RS (1972) *Inorg Chem* 11:1334–1338
- de Panthou FL, Belorizky E, Calemczuk R, Luneau D, Marcenat C, Ressouche E, Turek P, Rey P (1995) *J Am Chem Soc* 117:11247–11253
- Guedes GP, Zorzanelli RG, Comerlato NM, Speziali NL, Santos-Jr S, Vaz MGF (2012) *Inorg Chem Commun* 23:59–62
- Grand A, Rey P, Subra R (1983) *Inorg Chem* 22:391–394
- Caneschi A, Gatteschi D, Grand A, Laugier J, Pardi L, Rey P (1988) *Inorg Chem* 27:1031–1035
- Caneschi A, Gatteschi D, Laugier J, Rey P (1987) *J Am Chem Soc* 109:2191–2192

34. Gatteschi D, Laugier J, Rey P, Zanchini C (1987) *Inorg Chem* 26:938–943
35. Luneau D, Romero FM, Ziessel R (1998) *Inorg Chem* 37:5078–5087
36. Porter LC, Dickman MH, Doedens RJ (1986) *Inorg Chem* 25:678–684
37. Ullman FE, Osiecki JH, Boocock DGB, Darcy R (1972) *J Am Chem Soc* 94:7049–7059
38. Hirel C, Vostrikova KE, Pécaut J, Ovcharenko VI, Rey P (2001) *Chem Eur J* 7:2007–2014
39. Boudreaux EA, Mulay LN (1976) *Theory and application of molecular paramagnetism*. Wiley, New York
40. Gordon AB, John FB (2008) *J Chem Edu* 85:532–536
41. *SAINT-Plus*, version 6.02, Bruker Analytical X-ray System, Madison, WI (1999)
42. Sheldrick GM (1996) SADABS—an empirical absorption correction program; Bruker Analytical X-ray Systems, Madison, WI
43. Sheldrick GM (2015) SHELXTL refinement program version 2016/6. *Acta Crystallogr Sect C* 71:3–8
44. Osanai K, Okazawa A, Nogami T, Ishida T (2006) *J Am Chem Soc* 128:14008–14009
45. Okazawa A, Nogami T, Ishida T (2007) *Chem Mater* 19:2733–2735
46. Okazawa A, Nagaichi Y, Nogami T, Ishida T (2008) *Inorg Chem* 47:8859–8868
47. Okazawa A, Nogami T, Ishida T (2009) *Polyhedron* 28:1917–1921
48. Jiang ZH, Yi Q, Liao DZ, Huan ZW, Yan SP, Wang GL, Yao XK, Wang RJ (1995) *Trans Met Chem* 20:136–137
49. Caneschi A, Gatteschi D, Sessoli R, Hoffmann SK (1988) *Inorg Chem* 27:2390–2392
50. Wang XL, Li YX, Yang SL, Zhang CX, Wang QL (2017) *J Coord Chem* 70:1–10
51. Wang YL, Gao YY, Yang MF, Gao T, Ma Y, Wang QL, Liao DZ (2013) *Polyhedron* 61:105–111
52. Caneschi A, Ferraro F, Gatteschi D, Rey P, Sessoli R (1991) *Inorg Chem* 30:3162–3166
53. Fokin S, Ovcharenko V, Romanenko G, Ikorskii V (2004) *Inorg Chem* 43:969–977
54. Tretyakov E, Fokin S, Romanenko G, Ikorskii V, Vasilevsky S, Ovcharenko V (2006) *Inorg Chem* 45:3671–3678
55. Musin RN, Schastnev PV, Malinovskaya SA (1992) *Inorg Chem* 31:4118–4121

Publisher's Note Springer Nature remains neutral with regard to jurisdictional claims in published maps and institutional affiliations.